Available online at www.sciencedirect.com
ScienceDirect
Journal of Power Sources 161 (2006) 460–465
JOURNAL OF POWER SOURCES
www.elsevier.com/locate/jpowsour

High-rate electrochemical partial oxidation of methane in solid oxide fuel cells

Zhongliang Zhan [a], Yuanbo Lin [a], Manoj Pillai [b], Ilwon Kim [b], Scott A. Barnett [a,b,*]

[a] *Department of Materials Science and Engineering, Northwestern University, 2220 Campus Drive, Evanston, IL 60208, United States*
[b] *Functional Coating Technology LLC, 1801 Maple Ave., Evanston, IL 60201, United States*

Received 4 March 2006; received in revised form 21 April 2006; accepted 26 April 2006
Available online 30 June 2006

Abstract

This paper describes results on direct-methane solid oxide fuel cell (air, LSM-YSZ|YSZ|Ni-YSZ, CH_4) operation for combined electricity and syngas production. Thermodynamic equilibrium predictions showed that efficient methane conversion to syngas is expected for SOFC operating temperature >700 °C and O^{2-}/CH_4 ratios of ≈1. A simple thermal analysis was used to determine conditions where the cell produces enough heat to self-sustain its operating temperature; relatively low cell voltage and O^{2-}/CH_4 ratios > 1 were found to be useful. Fuel cells operated at $T \approx 750$ °C, $V \approx 0.4$ V, and $O^{2-}/CH_4 \approx 1.2$ yielded electrical power output of ∼0.7 W cm^{-2} and syngas production rates of ∼20 sccm cm^{-2}. Stable cell operation without coking for >300 h was achieved.

Keywords: Solid oxide fuel cell (SOFC); Methane; Syngas; Partial oxidation

1. Introduction

There have been a number of reports of the use of ceramic membrane reactors [1–4] and solid oxide fuel cells (SOFCs) [5–10] for methane partial oxidation (POx). Both these approaches seek to combine the POx catalytic reaction with electrochemically produced pure oxygen (i.e. electrochemical partial oxidation, or EPOx), thereby yielding syngas without nitrogen dilution. Syngas is an important precursor to synthetic liquid chemicals/fuels including methanol and various hydrocarbons [11–13]. The relative advantages and disadvantages of different methods for converting methane to syngas and other chemicals have been discussed in detail [11]. Key advantages of membrane or fuel cell reactors, compared to POx reactors that utilize cryogenically produced oxygen, include the reduced cost of the combined reactor and the elimination of explosive methane–oxygen mixtures. Furthermore, it may be possible to avoid thermal gradients arising from the two-step catalytic reaction process [11] – complete oxidation followed by methane reforming – as there have been indications of direct partial oxidation in SOFC reactors [7,8].

EPOx reactors may also have advantages relative to methane steam reforming reactors, which require excess pressurized steam, have problems with Ni catalyst coking, require relatively large amount of excess heat, and generally produce syngas that is too hydrogen-rich for production of hydrocarbons [11]. Note that steam reforming can be used to convert methane to syngas internal to SOFCs. The syngas is then oxidized to H_2O and CO_2 by the SOFC as it produces electricity. Thus, such internal reforming SOFCs cannot produce both electricity and syngas. EPOx is distinct from this in that electricity is produced during the reforming process, rather than after reforming, such that syngas can be output as a useful chemical product.

In this paper we focus on the SOFC reactor approach. Since the desired overall reaction is partial oxidation:

$$CH_4 + O^{2-} = CO + 2H_2 + 2e^- \quad (-22\,\text{kJ at } 750\,^\circ\text{C}) \qquad (1)$$

total SOFC currents and methane flow rates are adjusted to yield an O^{2-}/CH_4 ratio ≈ 1. This is quite different than direct-methane SOFCs, where the aim is to produce electricity by completely oxidizing methane:

$$(1/4)CH_4 + O^{2-} = (1/4)CO_2 + (1/2)H_2O + 2e^- \quad (-200\,\text{kJ at } 750\,^\circ\text{C}) \qquad (2)$$

* Corresponding author. Tel.: +1 847 491 2447; fax: +1 847 491 7820.
E-mail address: s-barnett@northwestern.edu (S.A. Barnett).

0378-7753/$ – see front matter © 2006 Elsevier B.V. All rights reserved.
doi:10.1016/j.jpowsour.2006.04.139

Comparison of reactions (1) and (2) shows that for a given sized SOFC (i.e. that transports a given amount of O^{2-}), the same amount of electricity ($2e^-$) is produced, while the methane feed rate and the products are different. This SOFC EPOx approach has two potential advantages over other syngas production methods. First, two useful products, syngas and electricity, are produced; in contrast, conventional SOFCs produce only electricity and ceramic membranes produce only syngas. Thus, there is the potential for improved economics relative to these methods. In this regard, it is necessary that the methane SOFCs provide competitive power densities similar to state-of-the-art electricity-only SOFCs, and similar syngas production rates as membrane reactors. However, in many prior results [5,7,8], SOFC power densities and syngas production rates were quite low. A second advantage is that EPOx can potentially build on an increasingly well-developed SOFC technology. However, this latter point is an advantage only if the SOFCs being developed for electricity generation can be adapted with minor changes to use methane instead of hydrogen. Unfortunately, prior demonstrations of EPOx involved SOFCs quite different than those being actively developed as electrical power sources. For example, the most successful demonstrations have been made with $(La,Sr)(Ga,Mg)O_3$ electrolyte SOFCs [6,10] rather than the more standard YSZ electrolytes, and methane conversion was relatively low. Other issues with prior EPOx SOFC reports are that methane diluted with, e.g., N_2 or He was used rather than pure methane, and life tests were limited to ~10 h. This latter point is especially important given the possible problem with coking in direct-methane SOFCs [14].

Here we present experimental results on EPOx carried out in planar Ni-YSZ anode-supported SOFCs operated with pure methane that provide high power densities, high syngas production rates, and high methane conversion. The SOFCs were similar to those being widely developed for electrical-generation applications, with the primary modification being the addition of a barrier layer at the SOFC anode. Stable operation without coking was demonstrated for a few hundred hours. Thermodynamic calculations of expected products are presented and used to estimate the thermal balance in EPOx SOFCs, and used as a guide for SOFC operating conditions.

2. Experimental procedures

2.1. Equilibrium calculation

A thermodynamic calculation described previously [15], similar to that reported by Koh et al. [16], was used to predict the expected equilibrium products versus O^{2-}/CH_4 ratio and temperature. The calculation minimizes the total Gibbs free energy of all species with the conservation of all elements in the system, starting with handbook values of the standard free energies [17]. A program based upon Taylor's expansion and Lagrange's method of undetermined multipliers was coded to solve the problem of minimization with constraints. In order to better match the present experimental results and prior work showing no carbon in direct-methane SOFCs [18–23], solid C was not allowed.

2.2. Fuel cell and barrier layer preparation

The SOFCs used in this study were fabricated as reported previously [24], consisting of Ni-YSZ anode supports (YSZ = 8 mol% Y_2O_3-stabilized ZrO_2), thin YSZ electrolytes, and LSM-YSZ cathodes ($LSM = La_{0.8}Sr_{0.2}MnO_3$). The anode substrates were pressed from NiO and YSZ (50/50, w/w) powders with 10% starch filler, and then bisque fired at 1100 °C. A NiO-YSZ anode active layer and a thin dense YSZ electrolyte layer were deposited on the NiO-YSZ supports using a colloidal deposition technique similar to that described previously [25]. The anode/electrolyte bi-layers were fired at 1400 °C for 6 h. LSM-YSZ cathode layers were applied and fired at 1250 °C for 1 h. Then a second layer of pure LSM slurry was applied and fired at 1250 °C for 1 h. The final fuel cells were ~2.5 cm in diameter, with anode thickness of ~0.6 mm, electrolyte thickness of ~10 μm, and cathode thickness of 20–30 μm. Estimated anode porosity was ≈40%, and cathode porosity was ≈30%. The cathode area, which defined the cell active area, was ~2.4 cm^2.

In some cases as noted below, a barrier or catalyst layer was placed adjacent to the SOFC anode. These were thin porous discs ≈0.3 mm thick consisting of partially stabilized zirconia. When a catalyst was used, it was a ≈15 μm thick Ru (10%)-CeO_2 layer screen printed on both sides. The addition of a barrier, or barrier with catalyst, helped to reduce the parameter range under which coking could occur [26,27].

2.3. Fuel cell testing and mass spectrometer measurement

Methane was used here as a well-controlled surrogate for natural gas. Methane is the primary constituent of natural gas, which also contains varying amounts (typically a few percent) of higher hydrocarbons and a small amount (a few ppm) of sulfur compounds. We have previously shown that the higher hydrocarbons in natural gas do not significantly alter SOFC operation compared with pure methane [20]. Sulfur impurities present in natural gas are typically removed prior to use in fuel cells [28]. Thus, differences between the present methane results and those for natural gas are expected to be minor.

Single cells were tested in a tube furnace using a standard testing geometry as illustrated in Fig. 1. A slightly modified test setup, where an alumina ceramic disc was attached to the end of the gas feed tube, was used in some of the tests. Ambient air was maintained on the cathode side. After reducing the anode NiO to Ni and initial electrical testing in humidified hydrogen, electrical

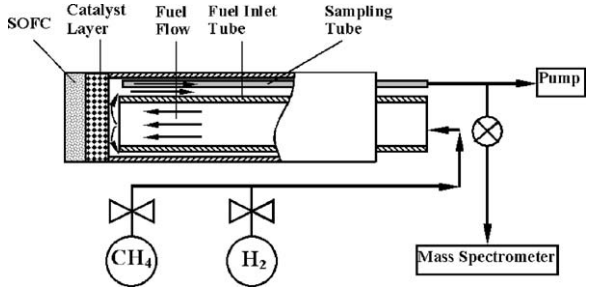

Fig. 1. Schematic of fuel cell testing setup.

measurements were done in pure methane. The fuel exhaust gas was sampled via a capillary tube with inlet placed near the anode, and was analyzed using a Transpector 2® Gas Analysis System (Inficon L100, electron impact ionization using 40 eV electrons) that was differentially pumped to a measurement pressure of $\approx 5 \times 10^{-5}$ Torr using a turbomolecular pump. Note that H_2O was removed from the products using a dessicant in order to avoid poisoning of the mass spectrometer.

3. Results and discussion

3.1. Equilibrium calculations

Predicted equilibrium products versus the O^{2-}/CH_4 ratio at a typical SOFC operating temperature of 750 °C are shown in Fig. 2. H_2 and CO increase with increasing O^{2-}/CH_4 to a maximum at $O^{2-}/CH_4 \approx 1$, while CH_4 decreases and H_2O and CO_2 remain relatively low. For $O^{2-}/CH_4 \approx 1$, the products agree reasonably well with Eq. (1). When the O^{2-}/CH_4 ratio is increased above ≈1, H_2 and CO decrease while H_2O and CO_2 increase, eventually reaching the composition given by Eq. (2) at $O^{2-}/CH_4 = 4$.

Equilibrium calculations were also used to estimate conditions where the EPOx SOFC reactor can be thermally self-sustaining. A minimum condition for this is that the net reaction enthalpy change $-\Delta H$ should equal the energy extracted as electricity (E_{FC}):

$$-\Delta H = E_{FC} \tag{3}$$

Note that the exothermic enthalpy change in partial oxidation, $-\Delta H_{PO} = 22\ \text{kJ mol}^{-1}$ CH_4 at 750 °C, is small relative to the expected electrical output $E_{FC} = nFV = 135\ \text{kJ mol}^{-1}$ CH_4 assuming a typical SOFC operating voltage $V = 0.7$ V (here $n = 2$ is the number of electrons in Eq. (1) and F is Faraday's constant). This situation can be improved by reducing the operating voltage, such that less electrical energy is extracted per mole of methane. Another measure that can be used to produce more heat is to increase O^{2-}/CH_4 above 1, which increases the amount of H_2O and CO_2 produced with substantial additional heat release

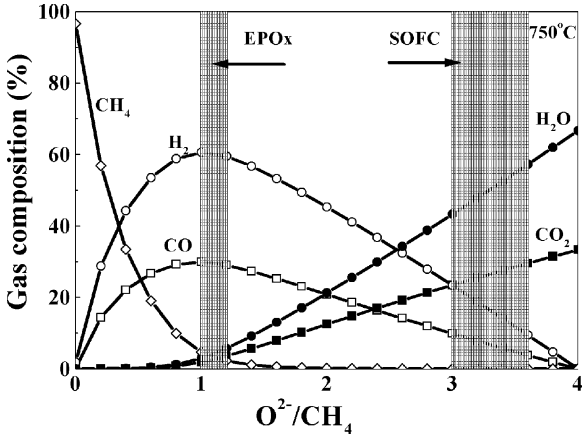

Fig. 2. Predicted equilibrium fuel gas composition vs. O^{2-}/CH_4 ratio at $T = 750$ °C, with the assumption that solid carbon does not form.

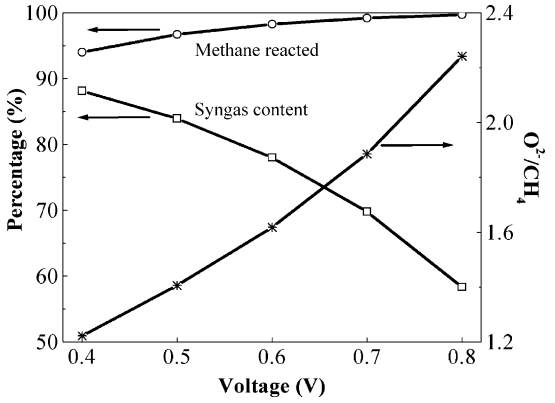

Fig. 3. O^{2-}/CH_4 ratio predicted to yield thermo-neutral SOFC operation vs. cell operating voltage at 750 °C. Also shown are the percentage of methane reacted and the syngas content of the product for the thermo-neutral condition.

(see Eq. (2)). Fig. 3 shows a plot of the O^{2-}/CH_4 and cell operating voltage values that satisfy Eq. (3) at 750 °C, where ΔH was calculated using the predicted equilibrium product composition. The results are approximate because heat losses, e.g. due to imperfect heat exchangers and a non-adiabatic reactor, were not included in Eq. (3). Fig. 3 shows that a lower V allows operation at lower O^{2-}/CH_4 values, e.g. 1.22 at 0.4 V versus 1.89 at 0.7 V at 750 °C. Fig. 3 also shows that decreasing V and O^{2-}/CH_4 increases the predicted syngas content of the products, e.g. from 70% at $V = 0.7$ V to 88% at $V = 0.4$ V, mainly due to a decrease in H_2O and CO_2, although the amount of un-reacted methane increases slightly. Calculations done at different temperatures, assuming thermo-neutral conditions (i.e. satisfying Eq. (3)) and $V = 0.4$ V, predicted high syngas productivity and methane conversion with relatively low H_2O and CO_2 content for temperatures > 700 °C.

The operation of a SOFC at $V = 0.4$ V would normally be expected to yield low fuel efficiency. The EPOx mode of operation is quite different, however, because the net fuel cell reaction is essentially partial oxidation, with a relatively low value of ΔH (see Eqs. (1) and (2)) compared to the essentially complete oxidation in a normal fuel cell. Thus, the net fuel cell efficiency, defined as $E_{FC}/\Delta H = nFV/\Delta H$, can be relatively high even for unusually low voltage. Another way of arguing this is the following: while the electrical energy output per mole of methane is relatively small, there is considerable energy value in the syngas produced that should also be considered in calculating efficiency.

3.2. SOFC electrical test results

Fig. 4 illustrates typical SOFC results for voltage V and power density P versus current density J, measured at 750 °C. Note that the O^{2-}/CH_4 ratio, also shown, was proportional to J since the CH_4 flow rate was fixed at 30 sccm. The cell performance was not measured at lower current density due to the risk of coking under these conditions [23]. V decreased with increasing J, while P increased to a maximum of 0.75 W cm^{-2} at $J \approx 1.6$ A cm^{-2} before decreasing at higher J. Fig. 4 shows that V values as low as 0.4 V, beneficial from the thermal balance viewpoint as shown in Fig. 3, can be used without compromising SOFC power density.

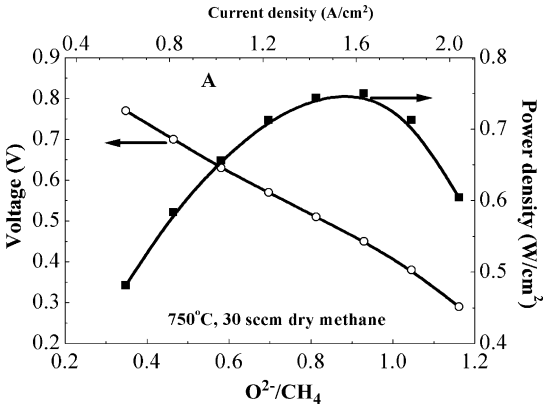

Fig. 4. Voltage and power density vs. current density (and O^{2-}/CH_4 ratio) for the SOFC NiO-YSZ|YSZ|YSZ-LSM, LSM, tested in 30 sccm dry methane in the anode and ambient air in the cathode at 750 °C.

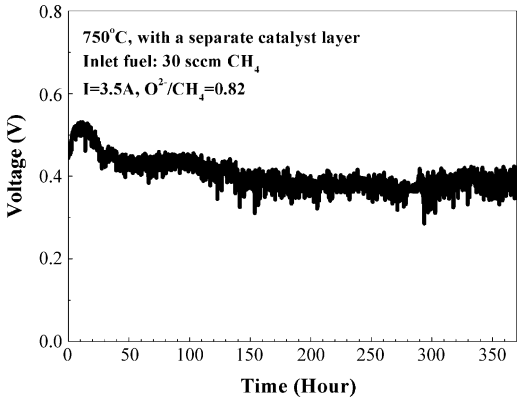

Fig. 5. Voltage vs. time for the SOFC, Ni-YSZ|YSZ|LSM-YSZ, LSM, with a catalyst layer, Ru-CeO_2|PSZ|Ru-CeO_2, and 3.5 A (O^{2-}/CH_4 = 0.82).

Fig. 4 also illustrates another advantage of lower V: decreasing from a typical SOFC voltage V = 0.7–0.4 V approximately doubles the oxygen ion current density J and the syngas production rate (the latter from Eq. (1)).

The present way of operating a SOFC, with pure methane fuel, low V, and high J, is unusual, so it is important to demonstrate that the cells can operate stably. Endurance tests carried out on a number of cells showed stable operation. Fig. 5 shows an example of a >300 h SOFC life test. The test was carried out with an anode catalyst layer using dry methane at 30 sccm, O^{2-}/CH_4 = 0.82, $V \approx 0.4$ V, and 750 °C. The SOFC showed a slight performance decrease during the first 150 h, followed by stable operation for the final 200 h at ≈0.6 W cm^{-2}. The initial performance decrease may have resulted from the relatively high current density, as a prior direct-methane life test at lower current and 700 °C showed no initial degradation [23]. Fig. 6 shows scanning electron microscope (SEM) images and energy-dispersive X-ray (EDX) analysis of the SOFC anode. The anode

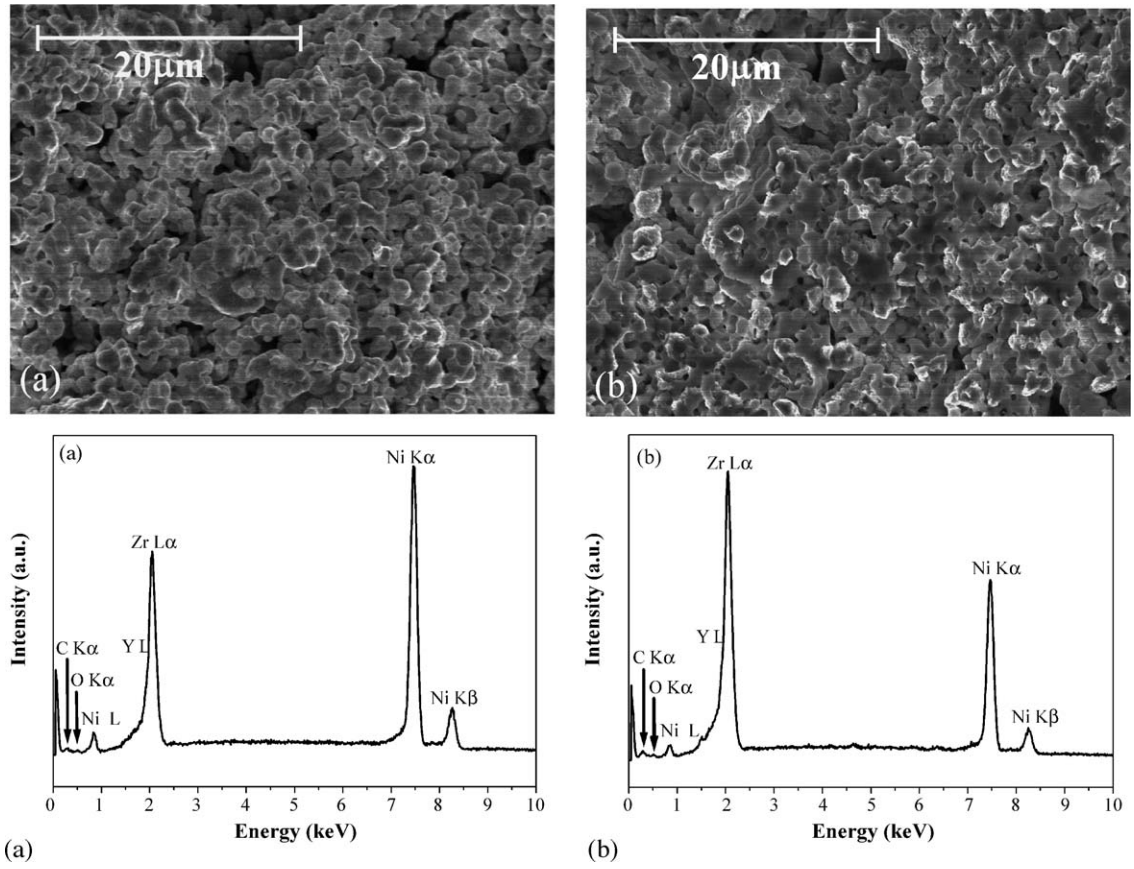

Fig. 6. Fracture cross-sectional SEM micrographs and EDX spectra taken from anodes after stable SOFC operation in (a) humidified hydrogen and (b) dry methane at 750 °C and J = 1.46 A cm^{-2}.

microstructure showed no evidence of any changes relative to a cell tested under conventional SOFC conditions in H_2 fuel, and the EDX spectra showed only a small carbon peak that was near the background level and similar to that for a cell tested with H_2 fuel. That is, no carbon was detected on the anode within the sensitivity of the measurement. Further life testing over longer time frames is needed to fully demonstrate stable SOFC operation under EPOx conditions.

3.3. Product gas composition

Fig. 7 shows typical mass spectra of the anode reaction products for SOFCs operated on methane at 750 °C and three different current densities. The spectrum at open circuit (Fig. 7a) shows main peaks at mass 2 (H_2^+), 15 (CH_3^+), and 16 (CH_4^+), reasonably corresponding to the input gas composition. The small H_2^+ peak was presumably due to methane cracking, indicating that solid C was depositing; this low J condition was generally avoided to prevent the deleterious C deposition [23]. Slight gas leakage in the fuel cell seals may explain small peaks at mass 28 (N_2^+ and CO^+) and 44 (CO_2^+). Overall, there was no apparent partial oxidation reaction at open circuit ($O^{2-}/CH_4 = 0$). At non-zero J values, peaks at mass 2 (H_2^+), 28 (CO^+), and 44 (CO_2^+) increased substantially while the CH_3^+ and CH_4^+ peaks decreased relative to Fig. 7a, as shown for $O^{2-}/CH_4 = 0.7$ (Fig. 7b) and $O^{2-}/CH_4 = 1.16$ (Fig. 7c).

Fig. 8 summarizes results as shown in Fig. 7. H_2 and CO increased to maximum values at $O^{2-}/CH_4 \approx 0.7$ before

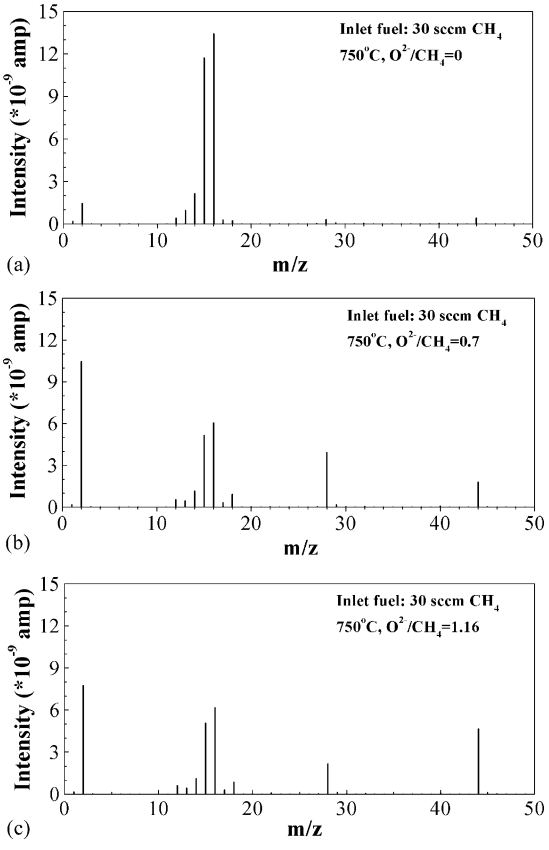

Fig. 7. Typical mass spectra of SOFC reaction products at 750 °C for 30 sccm dry methane at O^{2-}/CH_4 values of: (a) 0, (b) 0.7 and (c) 1.16.

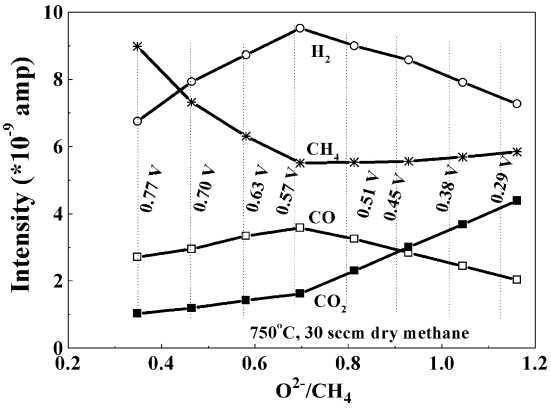

Fig. 8. The product gas peak intensity vs. O^{2-}/CH_4 ratio measured during the test shown in Fig. 4.

decreasing with further increases in O^{2-}/CH_4. The CH_4 content decreased with increasing O^{2-}/CH_4. The CO_2 content remained low at low O^{2-}/CH_4 but then increased more rapidly when O^{2-}/CH_4 increased above 0.7. These trends agree with the equilibrium prediction given in Fig. 1, except that CH_4 does not decrease to zero at large O^{2-}/CH_4, and the peak H_2 and CO content appears well below the predicted value $O^{2-}/CH_4 = 1$. Both these differences can be explained if a fraction of inlet CH_4 flow does not react, possibly due to the flow geometry of our SOFC test (Fig. 1).

In order to test the above explanation, we did additional experiments with an altered geometry where all CH_4 flowed over the full radius (~1 cm) of the anode. Fig. 9 shows schematically the original and modified geometries, and plots the methane utilization versus O^{2-}/CH_4 for both cases. In the new geometry, an annulus was used with a small hole at the center and a diameter nearly equal to the inside diameter of the test chamber. The new geometry also featured a reduced distance (≈1 mm versus ≈10 mm in the old setup) between the fuel inlet and the SOFC. These changes were made to force the fuel to flow radially across the surface of the anode, a geometry similar to radial-flow SOFC stack geometries. While fuel channel geometry in a stack will be constrained by other considerations (e.g. system issues such as

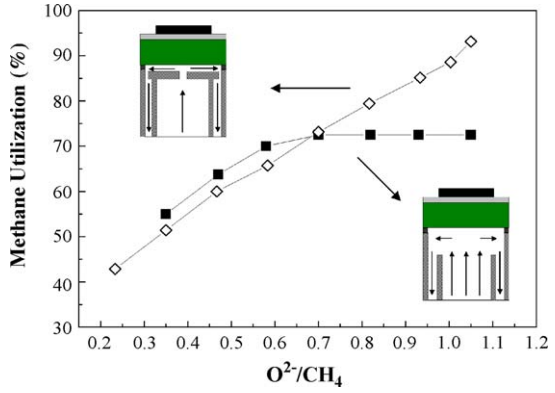

Fig. 9. Methane utilization vs. O^{2-}/CH_4 ratio for SOFCs operated on 30 sccm dry methane at 750 °C. Results are compared for identical SOFCs with the standard (■) and modified (◊) gas-flow geometries indicated schematically in the insets (the arrows illustrate the fuel flow path).

desired fuel pressure gradient), our methane conversion results were not strongly dependent on channel width; thus, it should be possible to achieve high methane conversion for reasonable stack fuel channel geometries. Fig. 9 shows that the methane utilization saturated at ≈70% for the original geometry, but for the altered geometry increased continuously to ≈90% for O^{2-}/CH_4 increased to 1. In the new geometry, the H_2 and CO mass spectrometer peaks increased continuously with increasing O^{2-}/CH_4 in this range, in better agreement with the thermodynamic prediction than in Fig. 8. The maximum measured syngas production rate estimated based on mass spectrometer sensitivities was $\sim 20\,\mathrm{sccm\,cm^{-2}}$.

While the products in Fig. 8 indicate partial oxidation of methane, it is not clear that the POx reaction occurred via a simple one-step process. Catalytic methane POx typically occurs by a two-step process, complete oxidation followed by reforming [11]. On the other hand, some SOFC EPOx results suggest a single-step POx reaction [7,8]. Visual observations of the cells during operation did not show evidence of substantial temperature gradients, as might be expected for a two-step process [11]. However, even in the case of a two-step process, the oxidation and reforming reactions may occur in close proximity yielding no substantial temperature gradients. The present results thus do not provide a definitive answer regarding reaction mechanism.

4. Conclusions

We have demonstrated that Ni-YSZ anode-supported SOFCs operated with pure methane fuel can produce both syngas and electricity without coking. The results show that SOFCs operated at $T \approx 750\,^{\circ}\mathrm{C}$, $V \approx 0.4\,\mathrm{V}$, and $O^{2-}/CH_4 \approx 1.2$ yield stable high electrical power output ($\sim 0.7\,\mathrm{W\,cm^{-2}}$) and high syngas production rates ($\sim 20\,\mathrm{sccm\,cm^{-2}}$). Equilibrium calculations suggest that the SOFC reactor should be thermally self-sustaining under these conditions.

Acknowledgement

This material is based upon work supported by the Department of Energy National Energy Technology Laboratory under Award Number DE-FC26-05NT42625.

References

[1] U. Balachandran, et al., Ceramic membrane reactor for converting methane to syngas, Catal. Today 36 (1997) 265–272.
[2] P.N. Dyer, R.E. Richards, S.L. Russek, D.M. Taylor, Ion transport membrane technology for oxygen separation and syngas production, Solid State Ionics 134 (2000) 21–33.
[3] S. Hamakawa, et al., Methane conversion into synthesis gas using an electrochemical membrane reactor, Solid State Ionics 136–137 (2000) 761.
[4] H.J.M. Bouwmeester, Dense ceramic membranes for methane conversion, Catal. Today 82 (2003) 141–150.
[5] G.L. Semin, V.D. Belyaev, A.K. Demin, V.A. Sobyanin, Methane conversion to syngas over Pt-based electrode in a solid oxide fuel cell reactor, Appl. Catal. Gen. 181 (1999) 131–137.
[6] T. Ishihara, T. Yamada, T. Akbay, Y. Takita, Partial oxidation of methane over fuel cell type reactor for simultaneous generation of synthesis gas and electric power, Chem. Eng. Sci. 54 (1999) 1535–1540.
[7] V.V. Galvita, V.D. Belyaev, A.K. Demin, V.A. Sobyanin, Electrocatalytic conversion of methane to syngas over Ni electrode in a solid oxide electrolyte cell, Appl. Catal. A: Gen. 165 (1997) 301–308.
[8] V.A. Sobyanin, V.D. Belyaev, Gas-phase electrocatalysis: methane oxidation to syngas in a solid oxide fuel cell reactor, Solid State Ionics 136–137 (2000) 747–752.
[9] H.-E. Vollmar, C.-U. Maier, C. Nölscher, T. Merklein, M. Poppinger, Innovative concepts for the coproduction of electricity and syngas with solid oxide fuel cells, J. Power Sources 86 (2000) 90–97.
[10] X. Zhang, S. Ohara, H. Chen, T. Fukui, Conversion of methane to syngas in a solid oxide fuel cell with Ni-SDC anode and LSGM electrolyte, Fuel 81 (2002) 989.
[11] H. Jack, Lunsford, Catalytic conversion of methane to more useful chemicals and fuels: a challenge for the 21st century, Catal. Today 63 (2000) 165–174.
[12] J.R. Rostrup-Nielsen, Syngas in perspective, Catal. Today 71 (2002) 243–247.
[13] D.J. Wilhelm, D.R. Simbeck, A.D. Karp, R.L. Dickenson, Syngas production for gas-to-liquids applications: technologies, issues and outlook, Fuel Process. Technol. 71 (2001) 139–148.
[14] C.M. Finnerty, N.J. Coe, R.H. Cunningham, R.M. Ormerod, Carbon formation on and deactivation of nickel-based/zirconia anodes in solid oxide fuel cells running on methane, Catal. Today 46 (1998) 137–145.
[15] Z. Zhan, J. Liu, S.A. Barnett, Appl. Catal. A: Gen. 262 (2004) 255–259.
[16] J.H. Koh, B.S. Kang, H.C. Lim, Y.S. Yoo, Electrochem. Solid State Lett. 4 (2) (2001) A12–A15.
[17] I. Barin, Thermochemical Data of Pure Substances, VCH, Weinheim, 1989.
[18] S.A. Barnett, Direct hydrocarbon solid oxide fuel cells, in: W. Vielstich, A. Lamm, H. Gasteiger (Eds.), Handbook of Fuel Cells, vol. 4, Wiley, Hoboken, NJ, 2003, pp. 1098–1108.
[19] E.P. Murray, T. Tsai, S.A. Barnett, A direct-methane fuel cell with a ceria-based anode, Nature 400 (1999) 649–651.
[20] J. Liu, S.A. Barnett, Operation of anode-supported solid oxide fuel cells on methane and natural gas, Solid State Ionics 158 (2003) 11–16.
[21] C. Xia, F. Chen, M. Liu, Electrochem. Solid State Lett. 4 (2001) A52.
[22] K. Ukai, Y. Mizutani, Y. Kume, O. Yamamoto, in: H. Yokokawa, S.C. Singhal (Eds.), Solid Oxide Fuel Cells VII, Electrochemical Society Proceedings Series, Electrochemical Society, Pennington, NJ, 2001, p. 375.
[23] Y. Lin, Z. Zhan, S.A. Barnett, Direct operation of solid oxide fuel cells with methane fuel, Solid State Ionics 176 (2005) 1827–1835.
[24] Z. Zhan, S.A. Barnett, An octane-fueled solid oxide fuel cell, Science 308 (2005) 844–847.
[25] J.W. Stevenson, Solid oxide fuel cell development in PNNL, in: S.C. Singhal, M. Dokiya (Eds.), Proceedings of the Eighth International Symposium on Solid Oxide Fuel Cells, Electrochemical Society, Pennington, 2003, pp. 31–39.
[26] Z. Zhan, Y.B. Lin, S.A. Barnett, Anode catalyst layers for direct hydrocarbon and internal reforming SOFCs, in: S.C. Singhal, J. Mizusaki (Eds.), Proceedings of the Ninth International Symposium on Solid Oxide Fuel Cells, Electrochemical Society, Pennington, 2005, pp. 1321–1330.
[27] Y. Lin, S.A. Barnett, J. Power Sources, in press, corrected Proof, available online 14 February 2006.
[28] C.S. Song, Fuel processing for low-temperature and high-temperature fuel cells—challenges, and opportunities for sustainable development in the 21st century, Catal. Today 77 (2002) 17–49.